Automatic Lumen Contour Detection in Intravascular OCT Images using Otsu Binarization and Intensity Curve

Hye Min Kim, Seung Hwan Lee, Chungkeun Lee, Jong-Won Ha and Young-Ro Yoon, *Members, IEEE*

***Abstract* — This paper proposes an automatic method for the detection of lumen contours in intravascular OCT images with guide wire shadow artifacts. This algorithm is divided into five main procedures: pre-processing, an Otsu binarization approach, an intensity curve approach, a lumen contour position correction, and image reconstruction and contour extraction. The 30 IVOCT images from six anonymous patients were used to verify this method and we obtained 99.2% sensitivity and 99.7% specificity with this algorithm.**

I. Introduction

Optical coherence tomography (OCT) is a light-based imaging system that provides in vivo high-resolution (<20um) images of vessels, including the coronary arteries [1]. The cross-section images include morphological and pathological information of arteries such as plaque, lumen, and stent strut, etc. [2]. To supply the objective information of artery images to cardiologists, recent studies [1-6] have proposed several automatic methods for detecting the vessel wall and stent strut by analyzing OCT images [1]. However, the algorithms of these studies work well only in cleared OCT images without the guide wire shadow artifacts or else there are long computing times due to complicated techniques, such as the Wavelet Transform (WT) and Active Contour Models (ACM), etc. [1,2].

In this paper, we propose an automatic algorithm of lumen segmentation that is fast, accurate, and simple. The proposed approach evaluated intravascular OCT (IVOCT) images with guide wire shadows acquired by Severance Hospital in Korea. Our method accuracy has 99.2% sensitivity and 99.7% specificity.

This paper is consisted of three sections. A characteristic of IVOCT images and a proposed algorithm is presented in Section II. The discussion of algorithm results is shown in Section III. Finally, the conclusion is discussed.

This research was supported by the Bio & Medical Technology Development Program of the National Research Foundation (NRF) funded by the Ministry of Science, ICT & Future Planning (NRF-2006-2005304).

H. M. Kim, S. H. Lee, and Y. R. Yoon are with the Department of Biomedical Engineering, College of Health and Science, Yonsei University, Wonju 220-710, Korea (corresponding author Yoon to provide phone: 82-33-760-2809; fax: 82-33-763-1953; e-mail: yoon@yonsei.ac.kr).

C. K. Lee is with the Severance Biomedical Science Institute, College of Medicine, Yonsei University, Seoul 120-752, Korea (e-mail: chungkeun@yuhs.ac).

J. W. Ha is with the Division of Cardiology, Severance Cardiovascular Hospital, Severance Biomedical Science Institute, College of Medicine, Yonsei University, Seoul 120-752, Korea (e-mail: jwha@yuhs.ac).

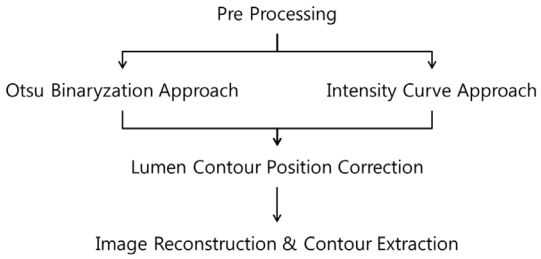

Figure 1. The process of contour detection algorithm

II. Materials and Methods

The process of the contour detection algorithm consists of five steps: pre-processing, an Otsu binarization approach, an intensity curve approach, a lumen contour position correction, and image reconstruction and contour extraction, as shown in Fig. 1. The two approaches subsequent to pre-processing are used to estimate the lumen contour. The material is composed of 30 IVOCT images from six anonymous patients. The images were acquired with a pullback of 20 mm/s, and 100 f/s, by a FD-OCT system (C7-XR, St. Jude Medical, Inc., Westford, Massachusetts, USA) and an image wire catheter (C7- dragonfly, St. Jude Medical, Inc.). Each image size is 1,024 by 1,024 pixels.

A. Pre-Processing

The size of image was reduced to 512 by 512 pixels because the original image size is too big to calculate. After converting the RGB image to a grayscale image, the catheter artifact is removed by eliminating the concerning pixels inside the catheter ring [2, 7], and the alignment marks are removed through a median filtering procedure [2] with a 10 by 10 window. Then, the polar transform was applied to IVOCT images because this transform converted the circular structure of the coronary artery to a straightened structure shown as Fig 4a. These straightened images were to improve the lumen detecting efficiency and simplify image descriptions [2, 7, 8].

B. Otsu Binarization Approach

Otsu Binarization Approach has five steps (Fig. 2). The polar image was divided into four segments and an Otsu thresholding algorithm was applied to each segment. Otsu [9] is a dynamic threshold selection method for dynamic binarization processes in which a histogram is divided into two classes, seeking the smallest variance between the two clusters. Hence, this provides a good separation for data with bimodal histograms [2]. Morphological opening, closing, and

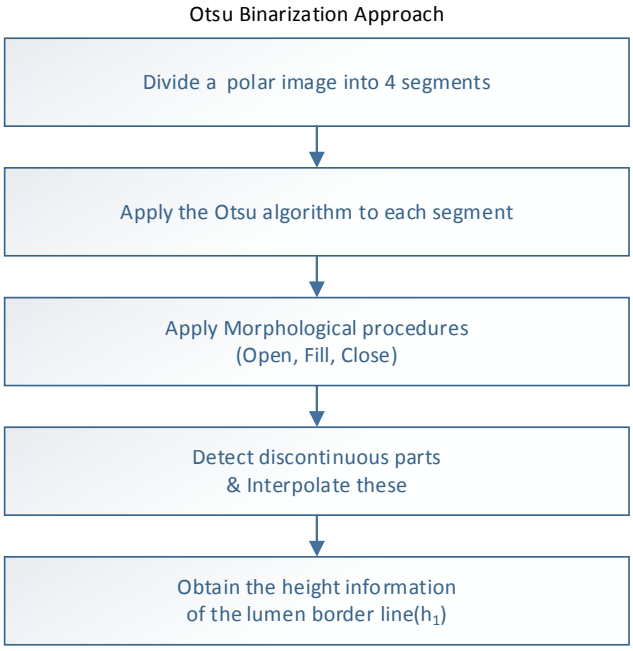

Figure 2. The process of Otsu binarization approach

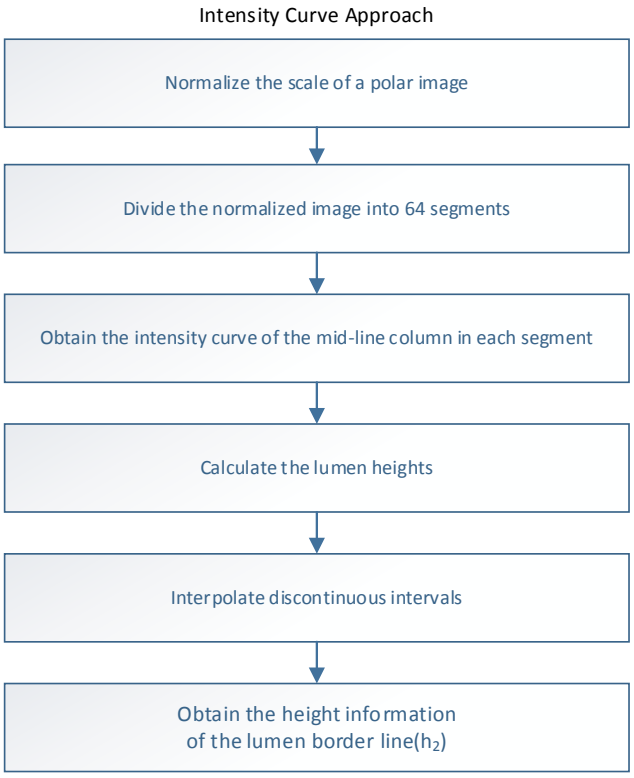

Figure 3. The process of intensity curve approach

filling procedures were applied to the binary image to reduce noise and refine the image.

There are discontinuous parts in the image caused by vessel bifurcations or catheter shadow. Therefore, detection of discontinuous parts and interpolation are necessary. In this method, the linear interpolation was used. Throughout this method, the height information of the lumen border line in the polar image (h_1) was obtained.

C. *Intensity Curve Approach*

The Otsu algorithm used in this study was a global binarization, thus, there might be errors in h_1. For this reason, another method was used to estimate the lumen border line for increasing accuracy. This method consists of six steps (Fig. 3). First, the polar image, which was obtained during the pre-processing step, was normalized to scale the range from 0 to 255. The normalized image was divided into 64 segments and the intensity curve of the mid-line column was obtained in each segment (Fig. 4). The lumen heights were calculated using the intensity curve. In the curve, if the maximum value of intensity is less than 100, this segment is counted as a discontinuous part. If the intensity value is more than 100, lumen height in each row is estimated. This estimation progresses the finding of the value of the row index, which has a maximum derivative value. Then, this row index is regarded as the lumen boundary point, meaning the height information of the lumen. If the intensity value is less than the average of the next five intensity values, this row might be media not intima. Thus, this index is also counted as a discontinuous part. To obtain the height information of the lumen contour in the polar image (h_2), the linear interpolation procedure is applied to every discontinuous interval. This interpolation makes 64 points of height information to 512 points.

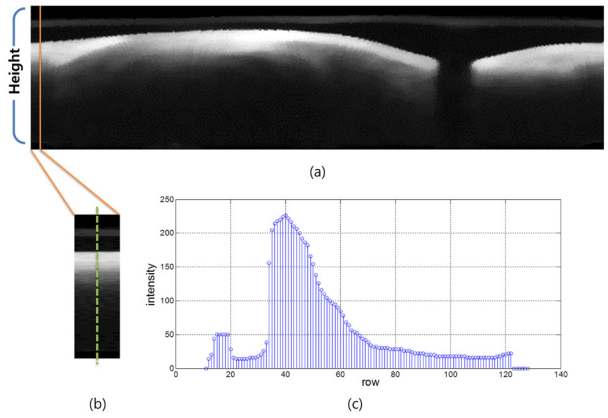

Figure 4. Intensity curve approach: (a) The normalized polar image; (b)The 1st segment of (a); (c) The intensity curve of mid-line column in (b)

D. *Lumen Contour Position Correction*

To obtain the accurate lumen contour, the selection procedure is carried out between h_1 and h_2. First, the indices,

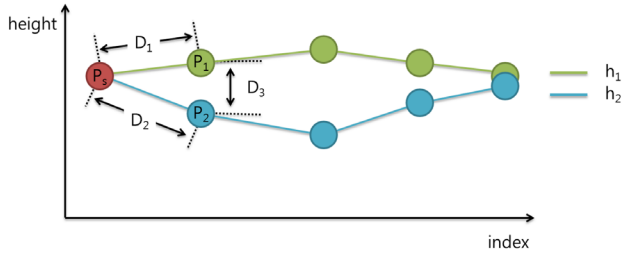

Figure 5. Lumen contour position correction: If th D_3 is less than 3 or D_1 is shorter than D_2, the next reference point will be P_1. Else if D_2 is shorter than D_1, the next reference point is P_2.

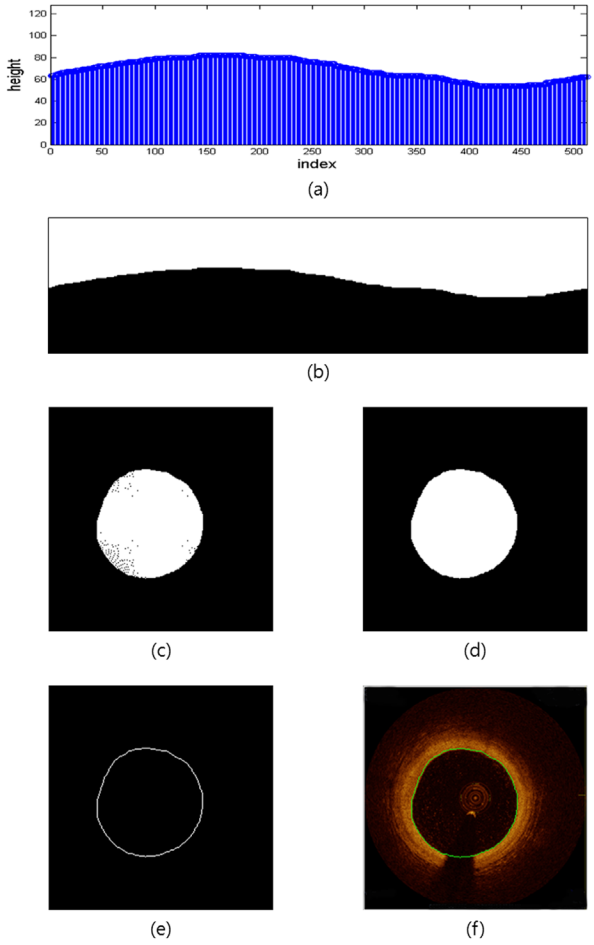

Figure 6. Image Reconstruction and Contour Extraction: (a) lumen height information; (b) reconstructed polar image; (c) converted Cartesian image; (d) closed Cartesian image; (e) extracted lumen contour; (f) OCT image and lumen contour

which have same value between h_1 and h_2, were found and the start point (P_s) was chosen. P_s is a reference point for selecting the next point. The point of the next index of P_s in h_1 and h_2, are P_1 and P_2, respectively. The distance between P_s and P_1 (D_1) and the distance between P_s and P_2 (D_2) were calculated (Fig. 5). If the difference (D_3) between the height values of P_1 and P_2 is less than 3 or D_1 is shorter than D_2, the next point is h_1 or else h_2 (Fig. 5), and this point is the next reference point. This procedure is repeated to obtain the correct lumen height information.

E. Image Reconstruction & Contour Extraction

The polar image (Fig. 6b) was reconstructed using the corrected lumen height information (Fig. 6a). The polar image was converted to a Cartesian domain (Fig. 6c) and the closing operation was carried out to fill the missing information in the Cartesian image (Fig. 6d). To extract the lumen contour, the erode operation was applied to the closed Cartesian image (Fig. 6e). Finally, the lumen contour was overlapped with the Cartesian OCT image (Fig. 6f).

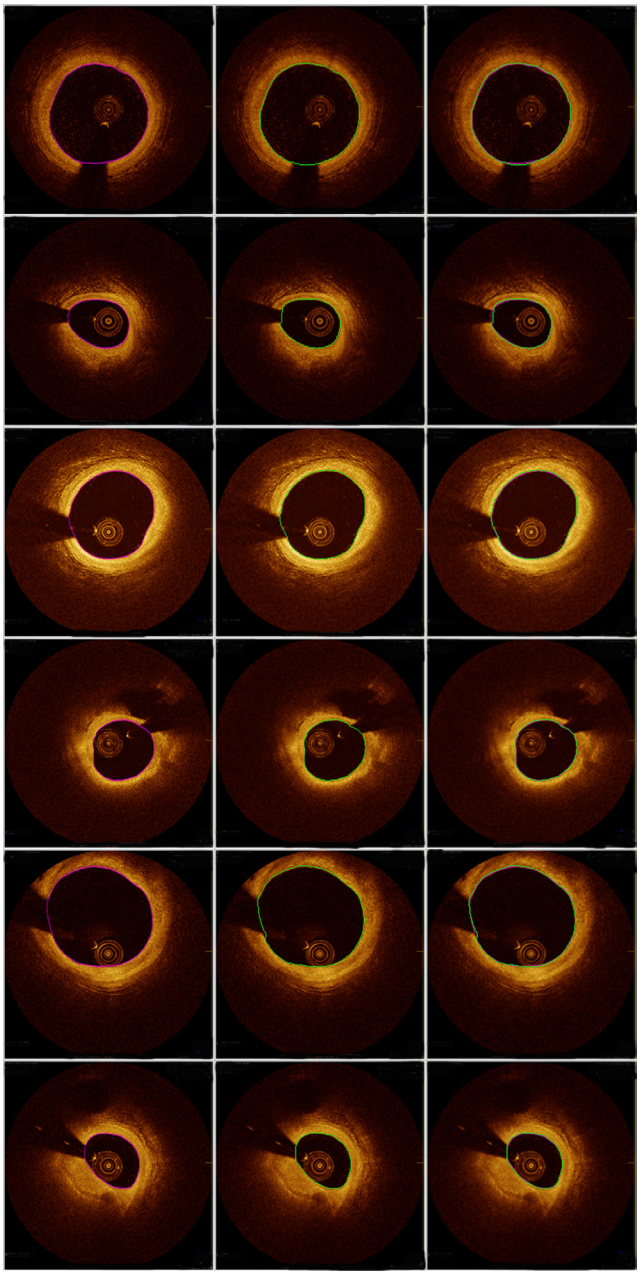

Figure 7. Lumen contour detection outcomes: The green line is the contour estimated by this method, and the magenta line is the gold standard. (Images of left column show the magenta line, images of mid column show the green line, and images of right column show both magenta and green lines)

III. Results and Discussion

The lumen detection was performed in a desktop computer with an Intel Core i7-4770 3.40 GHz, 8 GB of RAM, Windows 7 64 bits, and MATLAB (R2013a). The average time of the lumen contour detection was 0.367±0.005 s. This computational time is much faster than manual segmentation. In this paper, reference lumen contour, called gold standard as shown in Fig. 7, gotten by hand picking of clinical expert. This reference lumen contour had been compared with result of proposed method

TABLE I. ASSESSMENT OF ACCURACY[10]

Parameter	TPAF (%)	FPAF (%)	FNAF (%)	MaxFP (mm)	MaxFN (mm)
Average	99.21	0.30	0.79	0.15	0.11
Standard Deviation	±0.51	±0.15	±0.51	±0.03	±0.07

Pixel size: 15 um x 15 um

Image size: 512 x 512 pixels

The accuracy was obtained by computing average and standard deviations of the following five parameters: true positive area fraction (TPAF), the false positive area fraction (FPAF), the false negative area fraction (FNAF), the maximum false positive deviation (Max_{FP}), and the maximum false negative deviation (Max_{FN}) from 30 OCT images [2,10]. Fig. 7 shows the result of lumen contour detection and shows the accuracy of the algorithm in this study. In Table 1, the TPAF yielded more than 99%, the FPAF values came close to 0.3%, and the FNAF value was less than 0.08%. The specificity is defined by 1-FPAF and the sensitivity is defined by TPAF [10]. Therefore, the specificity and sensitivity of this method are 99.2% and 99.7%, respectively. The precision and robustness of this method can be seen through the standard deviation of the parameter results lower than 1%. The Max_{FP} and Max_{FN} are approximately 0.15mm and 0.11mm, respectively, for an image size of 15.36 mm by 15.36 mm.

Our proposed method was motivated by [2]. The paper, proposed by M. C. Moraes, et al., presents the accuracy of detecting lumen, but they used high computational methods as the Discrete Wavelet Packet Frame (DWPF). For reducing computational cost, DWPF was removed and image processes, including opening, closing, and filling, were lessened. The computational speed proposed by [2] was 5.9±3s, but our method used a speed of 0.367±0.005s, and the accuracy of lumen segmentation was excellent, even when compared with result of [2]. Although our test circumstances did not involve the same image or computer, the accuracy and robustness of the proposed method is supported by parameters (Table 1). In some resulting images, there are misdetections around guide wire shadow neighboring. These errors can be removed by applying improved interpolation techniques, such as cubic spline or radial basis function interpolation, instead of the linear interpolation used in this study.

IV. CONCLUSION

We presented an automatic method based on an Otsu binarization and a mathematical approach with an intensity curve for the lumen contour detection in IVOCT images that have guide wire shadow. This method does not have a complicated methodology, such as the Wavelet transform or active contour models. Therefore, the computing speed is faster than previously studied [1, 2]. However, the accuracy is better than in these studies or similar. Our method, therefore, estimates the lumen contour in the region affected by guide wire shadows accurately. The accuracy of lumen contour detection is expected to increase by modifying the finding point algorithm in the intensity curve and interpolation. In this study, we found only the lumen position in the intensity curve, but upon further study, we will find the end of the media position and calculate the External Elastic Membrane (EEM) automatically.

ACKNOWLEDGMENTS

The authors are grateful to colleagues of Bio Signal Processing laboratory in Yonsei graduate and department of interventional cardiology in Severance hospital, who have made important contributions to this work.

REFERENCES

[1] K. P. Tung, W. Z. Shi, R. D. Silva, E. Edwards, and D. Rueckert, "Automatical vessel wall detection in intravascular coronary OCT," *The IEEE International Symposium on Biomedical Imaging: From Nano to Macro*, pp. 610–613, 2011.

[2] M. C. Moraes, D. A. C. Cardenas, and S. S. Furuie, "Automatic lumen segmentation in IVOCT images using binary morphological reconstruction," *Biomedical engineering online*, vol. 12:78, 2013.

[3] F. Dubuisson, C. Kauffmann, P. Motreff, and L. Sarry, "In vivo OCT coronary imaging augmented with stent reendothelialization score," *Medical Image Computing and Computer-Assisted Intervention-MICCA/2009*, Springer Berlin Heidelberg, pp. 475–482, 2009.

[4] S. Gurmeric, G. G. Isguder, S. Carlier, and G. Unal, "A new 3-d automated computational method to evaluate in-stent neointimal hyperplasia in in-vivo intravascular optical coherence tomography pullbacks," *Medical Image computing and computer-assisted Intervention-MICCA/2009*, Springer Berlin Heidelberg, pp. 776–785, 2009.

[5] C. Kauffmann, P. Motreff, and L. Sarry, "In vivo supervised analysis of stent reendothelialization from optical coherence tomography," *IEEE Transactions on Medical Imaging*, vol. 29, no. 3, pp. 807–818, 2010.

[6] N. Gonzalo, *Optical coherence Tomography for the Assessment of coronary Atherosclerosis and Vessel Response after Stent Implantation*, Ph.D. thesis, Erasmus University Rotterdam, 2010.

[7] M. C. Moraes, S. S. Furuie, "Automatic coronary wall segmentation in intravascularultrasound images using binary morphological reconstruction," *Ultrasound in Medicine & Biology*, vol. 37, no. 9, pp. 1486–1499, 2011.

[8] M. Papadogiorgaki, V. Mezaris, Y. S. Chatzizisis, G. D. Giannoglou, I. Kompatsiaris, "Image analysis techniques for automated ivus contour detection," *Ultrasound in Medicine & Biology*, vol. 34, no. 9, pp. 1482–1498, 2008.

[9] N. Otsu, "A threshold selection method from gray-level histograms," *IEEE Trans Systems, Man, and Cybernetics*, vol. smc-9, no. 1, pp. 62–22, 1979.

[10] J. K. Udupa, V. R. LeBlanc, Y. Zhuge, C. Imielinska, H. Schmidt, L. M. Currie, B. E. Hirsch, and J. Woodburn, "A framework for evaluating image segmentation algorithms," *Computerized Medical Imaging and Graphics,* vol. 30, no. 2, pp. 75–87, 2006.